Macromolecules

pubs.acs.org/Macromolecules Article

Poly(3,4-epoxycyclohexylmethyl acrylate) Synthesis and Use in the Preparation of an Exceptionally Hard yet Flexible Organic Polymer Coating

Ryan Seck, Ziruo Lai, and Guojun Liu*

Cite This: Macromolecules 2024, 57, 11670–11678 Read Online

ACCESS | Metrics & More | Article Recommendations | Supporting Information

ABSTRACT: Despite the commercial availability of 3,4-epoxycyclohexylmethyl acrylate (ECMA), its homopolymerization is not reported. In this study, liquid viscous poly(3,4-epoxycyclohexylmethyl acrylate) (PECMA) is synthesized via free radical polymerization and fractionated to obtain samples with varying molecular weights. After casting with a cationic photoinitiator and photocuring of the resultant film to cross-link the epoxide groups via ring-opening polymerization, a hard solid coating is formed. For fully cured coatings, hardness (H) increases with the molecular weight of PECMA. At a weight-average molecular weight (M_w) of 14.5 kDa, the H value of the fully cured coating reached 0.78 ± 0.02 GPa, over five times that of poly(ethylene terephthalate) (PET) and three times that of polystyrene (PS), representing the highest H value reported for an organic material. This exceptional hardness correlates with excellent wear resistance, as no wear tracks are observed after 250 abrasion cycles with steel wool under 13 kPa. The coating also exhibits high transparency, with 97% transmittance at 500 nm for a 50 μm-thick film, and remains thermally stable up to 300 °C. These properties indicate that PECMA holds significant potential for diverse applications.

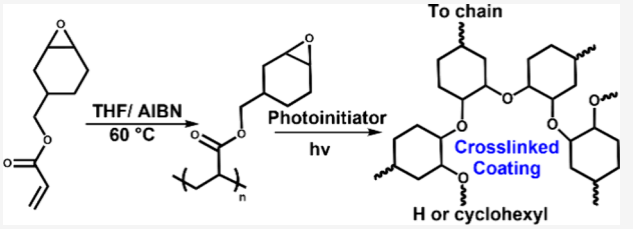

INTRODUCTION

A hard, wear-resistant, and transparent polymer has numerous potential applications, such as serving as an encapsulation layer for touch screens or as protective coatings for appliances. Traditionally, organic polymers fall short in terms of hardness, with nanoindentation hardness (H) values typically below 0.40 GPa.[1,2] For applications demanding high wear resistance, polymer/inorganic nano- and microcomposites are commonly employed.[3−7] Recently, research has focused on organic/inorganic hybrid polymers (molecular composites) to achieve these properties.[8−15] Despite advancements in resolving compatibility issues between organic and inorganic phases in polymer composites, an all-organic polymer that matches the hardness and wear resistance of composites or molecular composites would be highly advantageous. For example, a single polymer could be easier to handle and process than a composite mixture. Additionally, discovering polymers with exceptional hardness and wear resistance could open new research avenues. This paper presents a liquid or rubbery polymer that, upon photocuring, yields a solid or coating with an exceptionally high nanoindentation hardness of 0.78 ± 0.02 GPa, which is five times greater than that of poly(ethylene terephthalate) (PET) and three times greater than that of polystyrene (PS).

This polymer is derived from a bifunctional monomer, 3,4-epoxycyclohexylmethyl acrylate (ECMA, Scheme 1a). While the free radical polymerization of the double bond of ECMA allows the preparation of a linear polymer (a → b), the resultant polymer in a solvent containing a cationic photoinitiator triphenylsulfonium hexafluoroantimonate salts (TSHFA) can be cast to yield a liquid polymer film. Subsequent photocuring triggers the cationic ring-opening polymerization of the pendant epoxy groups (b → c), yielding a cross-linked hard coating.[16]

We investigated PECMA and its cross-linked resin because a ladder-like polysilsesquioxane with pendant epoxycyclohexyl groups exhibits impressive nanoindentation hardness (>1.4 GPa).[11,14,15] We hypothesize that these pendant groups may impart similar advantages to an organic polymer. Despite the commercial availability of ECMA and existing patent literature on its synthesis and purification,[17,18] we were surprised to find a lack of publications on the homopolymerization of ECMA to produce linear polymers. This absence may be due to the monomer's relative obscurity among academic researchers.

However, there is literature on ECMA's copolymerization with other monomers. For instance, Liu et al.[19] copolymerized ECMA with various monomers and then cross-linked the

Received: September 5, 2024
Revised: November 29, 2024
Accepted: December 4, 2024
Published: December 12, 2024

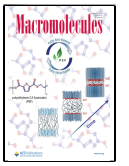

https://doi.org/10.1021/acs.macromol.4c02127
Macromolecules 2024, 57, 11670−11678

Scheme 1. Reactions for (a → b) PECMA Synthesis and (b → c) PECMA Cross-Linking

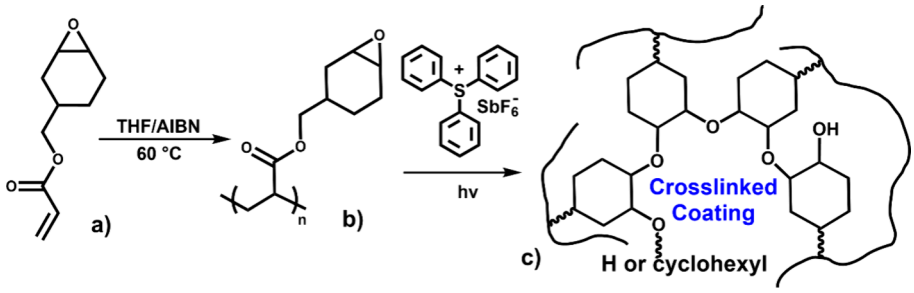

pendant epoxide rings to enhance their cohesive strength to facilitate pressure-sensitive adhesive application. Yamawake and Hayashi[20] employed reversible addition−fragmentation chain transfer polymerization to copolymerize ECMA with other monomers. The produced polymers were subsequently cross-linked with 2,2′-dithiodibenzoic acid via epoxide ring opening by the carboxyl groups. Since disulfide bonds are reversible, the cross-linked polymers exhibited self-healing properties.

Like ECMA, (3,4-epoxycyclohexyl)methyl methacrylate has primarily been featured in copolymerization literature. For instance, a copolymer was synthesized through the free radical copolymerization of this monomer with *tert*-butyl methacrylate.[21] After cross-linking with an anhydride and subsequently removing the *tert*-butyl groups, a porous material with a low dielectric constant and loss was produced.

Additionally, a cycloaliphatic epoxide-acrylate hybrid monomer was synthesized by reacting a diepoxy compound with a limited amount of acrylic acid, resulting in a monomer containing, on average, one epoxide ring per molecule.[22] A photoinitiator capable of generating both radicals and cations upon irradiation was then used to enable the simultaneous polymerization of the double bonds and epoxy groups, yielding a cross-linked polymer in a single step.

EXPERIMENTAL SECTION

Materials. ECMA (>94%, TCI) was purified by running it though a basic Al_2O_3 column. Tetrahydrofuran (THF, ≥99.0%, Sigma-Aldrich) was distilled before use. 2,2-Azobis(isobutyronitrile) (AIBN, 98%, Sigma-Aldrich), Al_2O_3 (activated, basic, Brockmann I, Sigma-Aldrich), hexanes (mixture of isomers, ≥98.5%, Sigma-Aldrich), 2-(3,4-epoxycyclohexyl)ethyl trimethoxysilane (ECTMS, 97%, Gelest), ethanol (anhydrous, 99.5%, Commercial Alcohols), acetic acid (glacial, Fischer Scientific), 2-propanol (≥99.5%, Sigma-Aldrich), 1,4-dioxane (>99%, Sigma-Aldrich), polystyrene (PS, average molecular weight M_w = 35 kDa, Sigma-Aldrich), $CDCl_3$ (99.8 atom % D, Sigma-Aldrich), and triphenylsulfornium hexafluoroantimonate salts (TSHFA, 50 wt % in propylene carbonate) were used as received. Glass slides (Fisher Scientific microscope slides, 7.62 cm × 2.54 cm) were cut using a diamond knife into 2.54 × 2.54 cm^2 squares and washed with acetone prior to use. Poly(ethylene terephthalate) (PET) sheets, 50 and 125 μm-thick, were both Dura-Lar clear films manufactured by Grafix, Inc.

ECMA Polymerization. AIBN (33.9 mg, 2.10 × 10^{-4} mol), anhydrous tetrahydrofuran (37.5 mL), and ECMA (7.7 g, 4.0 × 10^{-2} mol) were mixed in a 100 mL single-neck round-bottom flask containing a magnetic stirrer. After wrapping the protruding part of the rubber septum with Teflon tape, it was inserted into the flask's neck. The septum's sleeve was then turned onto the outer surface of the flask's neck. Finally, parafilm and electrical tape were applied over the sleeve to ensure a tight seal. The mixture was subsequently bubbled under N_2 for 15 min. The nitrogen was delivered by a long needle inserted through the septum with the tip submerged in the mixture. The gases were released from the flask simultaneously by a shorter needle, which was also inserted through the septum. After N_2 bubbling, the flask was heated for 12 h at 60 °C while being stirred at 850 rpm. After cooling to room temperature, the solution was added into excess hexanes to precipitate the formed polymer. The polymer was settled via centrifugation, and the supernatant was removed via decantation. The crude product was dissolved in THF and precipitated into hexanes again and purified. This purification cycle was repeated one time before the polymer was dried using rotary evaporation, yielding a sticky viscous liquid at a yield of 82%. The polymer was redissolved in THF as a solution to reduce viscosity, facilitating later handling.

PECMA Fractionation. To fractionate PECMA, hexanes were added dropwise under stirring into a PECMA solution in THF. Once the solution became slightly opaque, the flask was placed in a 4 °C fridge overnight to allow the separation of a polymer-rich layer from the supernatant. After the separation of the bottom phase, the solvent was removed for weight determination before it was redissolved in THF for storage. The fractionation process was repeated with the fractionated samples until PECMA samples with desired M_w and PDI were obtained when analyzed using SEC.

Coating Preparation. To manufacture 50 μm-thick coatings, PECMA was dissolved in 1,4-dioxane at a concentration of 118 g/mL. TSHFA in propylene carbonate was added using an Eppendorf pipet at mass percentage amounts of 0.50, 1.25, 2.0, and 5.0% in the final PECMA/TSHFA mixture. The solution mixture, 0.30 mL containing 35.5 mg of PECMA, was drop-cast onto a 2.54 cm × 2.54 cm ECTMS-treated slide. The density of PECMA was assumed to be the same as ECMA at 1.10 g/cm^3, as quoted by TCI America. The coating samples were placed in a N_2 oven and were allowed to sit for 8 h at room temperature before being heated at 60 °C for 9 h. After heating, the liquid polymer was seen to remain as an even film on the substrate. The coatings were photolyzed for 40 min using a focused beam from a 500 W mercury lamp that passed through a 280 nm cutoff filter. This process yielded solid 50 μm-thick PECMA coatings, which were transparent with yellow tint.

Thermogravimetric Analysis (TGA) and Differential Scanning Calorimetry (DSC). Cured PECMA samples were prepared on glass plates following standard coating protocols. Coating fragments were removed with a razor blade and placed into sample pans for analyses. For a photoinitiator-free sample, PECMA was dissolved in 1,4-dioxane (118.33 mg/mL), and 0.050 mL of this solution was dispensed into a DSC pan using a microsyringe. The solution was dried under nitrogen, first at room temperature for 8 h and then at 60 °C for 10 h.

TGA was conducted with a TGAQ500 instrument, and samples were heated to 100 °C at 10 °C/min, held for 5 min, and further heated to 600 °C at the same rate. DSC was performed with a DSCQ100 instrument, and the sample was cooled to −30 °C, heated to 50 °C at 5 °C/min, and cooled back to −30 °C at −5 °C/min. When the highest temperature was 100 °C, the heating and cooling rates used were 10 °C/min. The cycles were repeated twice.

https://doi.org/10.1021/acs.macromol.4c02127
Macromolecules 2024, 57, 11670−11678

RESULTS AND DISCUSSION

PECMA Synthesis. THF and dioxane were individually tested as solvents for the free radical polymerization of ECMA initiated with AIBN. Dioxane was eventually discarded as a solvent due to PECMA cross-linking. While we do not know the exact cross-linking mechanism, one possibility is the simultaneous polymerization of the epoxide rings via ring opening and of the double bonds via free-radical-catalyzed chain addition. The former can be triggered by a trace impurity in dioxane. Alternatively, cross-linking can be due to a well-known mechanism for acrylates involving the transfer of the radical centers from the terminal ends of growing polymer chains to polymer backbones and the subsequent recombination of the formed backbone radicals.[23]

For polymerization in THF, we tested different initiator and monomer concentrations, as well as polymerization times. We optimized the conditions to a THF-to-ECMA volume ratio of 5:1 and an AIBN molar concentration of 0.50% relative to the monomer. The polymerization was carried out at 60 °C for 12 h, achieving a 98% conversion of double bonds as determined by ^{1}H NMR analysis. Longer polymerization times were avoided to reduce the risk of ECMA cross-linking.

Figure 1 displays the SEC trace for a purified PECMA sample. The polydispersity index, determined via PS calibration, is 2.17, which is typical for free radical polymerization. The PS-equivalent weight-average molecular weight (M_w) of the sample is 10.4 kDa. This M_w is relatively low probably due to facile chain transfer to THF.[24] This transfer presumably also eliminated PECMA cross-linking. In the future, the molecular weight of PECMA could potentially be increased through the use of alternative solvents and further optimization of the polymerization conditions. We did not pursue higher M_w in this study, as the primary objective was to assess PECMA's potential as a hard resin or coating. We obtained higher-molecular-weight samples via fractionating the prepared PECMA.

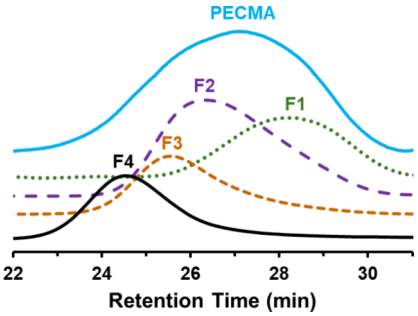

Figure 1. SEC traces of PECMA and its fractions F1, F2, F3, and F4.

The structure of the polymer was confirmed by NMR spectroscopy. Figure 2c presents the ^{1}H NMR spectrum of PECMA, which appears complex. To aid in the peak assignments, we first analyzed the NMR spectrum of ECMA, shown in Figure 2b. The complexity of the ECMA spectrum arises because the (3,4-epoxycyclohexyl)methyl acrylate is synthesized through the epoxidation of (3-cyclohexenyl)-methyl acrylate,[19] with oxygen potentially added to either side of the cyclohexenyl ring. This introduces chiral centers at carbons 3 and 4 (Figure 1a), resulting in three chiral centers (at carbons 1, 3, and 4) and four stereoisomers, which can be

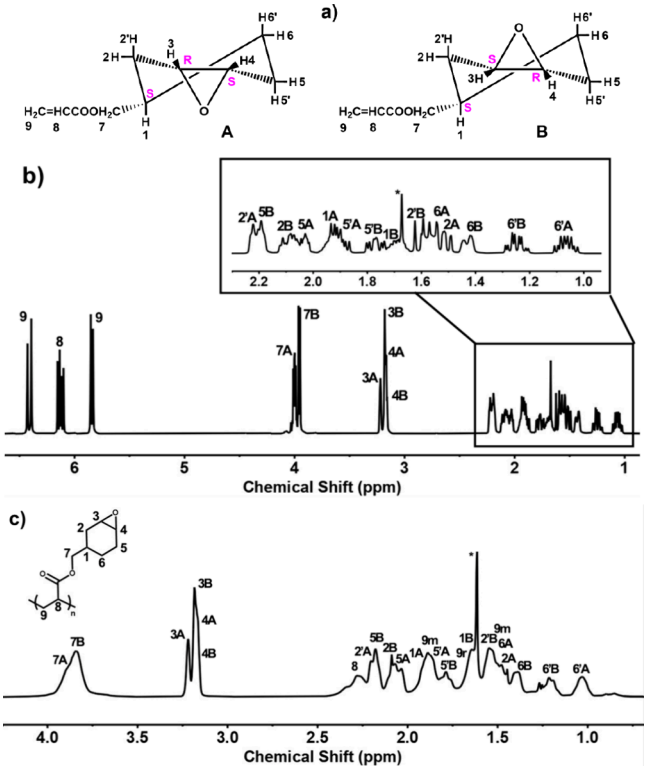

Figure 2. (a) Molecular structures and atomic numbering for A- and B-type stereoisomers of ECMA. Here, H# and H#' denote protons in equatorial and axial positions, respectively. Panels (b) and (c) show ^{1}H NMR spectra of ECMA and PECMA and peak assignments.

divided into two groups of diastereomers or two groups of enantiomers.

For ECMA peak assignments, a comprehensive set of NMR techniques, including ^{1}H, ^{13}C, DEPT, COSY, HSQC, and NOESY, were used. As the methods for peak assignments have been recently reported for 2-(3,4-epoxycyclohexyl)ethyl trimethoxysilane,[25] we will not discuss the results in detail here but summarize the assignments in Figure 2.

The major changes in the NMR spectra from ECMA to PECMA are the disappearance of vinyl proton peaks between 5.83 and 6.37 ppm (Figure S1), the appearance of new peaks for protons attached to the main chain carbons, and peak broadening. For the new peaks, there is an additional complication, i.e., the relative orientations of the pendant 3,4-epoxycyclohexylmethyl groups in PECMA can result in two adjacent ECMA units being either a *meso* (*m*) or *racemo* (*r*) diad. Consequently, the protons on carbon 9 (as depicted in Figure 2c) within these diads can exhibit slightly different chemical shifts, similar to the protons in the backbone of poly(methyl methacrylate).[26] Therefore, in Figure 2c, 9m and 9r denote the protons on carbon 9 in *meso* and *racemo* diads, respectively.

Accurate assignments of the ^{1}H NMR peaks for PECMA will enhance future studies. They allowed us to conclude that PECMA was synthesized under our conditions without any detectable cross-linking.

PECMA Fractionation. The synthesized PECMA underwent fractional precipitation to yield four fractions denoted as F1−F4 with different molecular weights. Figure 1 also shows the SEC traces for the four fractions investigated in this study. The PS-equivalent M_w and M_w/M_n values calculated from

https://doi.org/10.1021/acs.macromol.4c02127
Macromolecules 2024, 57, 11670−11678

these traces are listed in Table 1. The fractions are sharper in molecular weight distributions and cover M_w ranging from 4.1 to 29.9 kDa.

Table 1. Weight-Average Molecular Weights M_w and Polydispersity Indices M_w/M_n of PECMA and Its Fractions

sample	M_w (kDa)	M_w/M_n
PECMA	10.4	2.17
F1	4.1	1.50
F2	9.3	1.69
F3	14.5	1.64
F4	29.9	1.38

Surface Modification of Glass Slides. The PECMA coating on glass slides delaminated within a few days after photocuring. To enhance the adhesion of PECMA, we modified the glass surfaces with a coupling agent, 2-(3,4-epoxycyclohexyl)ethyl trimethoxysilane (ECTMS), using sol–gel chemistry. This treatment increased the water contact angle of the glass from 35 ± 1 to 72 ± 1°.

We analyzed the ATR-FTIR spectra of the glass plates before and after ECTMS treatment, as shown in Figure 3.

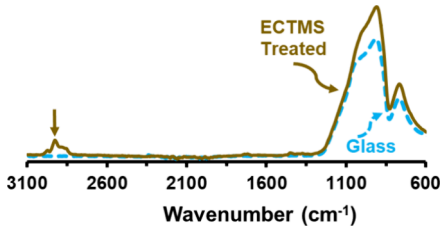

Figure 3. Comparison of ATR-FTIR spectra of a glass slide before and after ECTMS Treatment.

While the characteristic epoxide peaks between 750 and 1000 cm^{-1} are obscured by the O–Si peaks of the glass, the C–H stretching of the epoxide and ring is clearly observable at 2972 cm^{-1}, and the symmetric and asymmetric stretching of the CH_2 groups of the cyclohexane ring are observed at 2853 and 2927 cm^{-1}, respectively.[14,27] These results and the contact angle increase confirm the successful grafting of ECTMS onto the glass. Additionally, PECMA coatings on ECTMS-treated glass did not exhibit delamination within a month, further validating the effectiveness of the surface treatment.

Coating Preparation. The coatings were prepared via evaporating solvents from cast solutions of PECMA or its fractions containing TSHFA followed by photocuring the resultant films. To determine the residual amounts of THF and dioxane in a cast PECMA sample before photocuring, we conducted ^1H NMR analysis of it. The residual weight fractions of THF and dioxane in it were 0.71 and 0.73%, respectively, indicating effective solvent removal.

Figure 4a displays the ATR-FTIR spectrum of a 50 μm F2 coating sample prior to photocuring. This sample contained less than 1.5% solvents. To assess the solvent impact, we obtained the spectrum, as shown in Figure S2, of an F2 sample dried under vacuum at 60 °C for 8 h, rather than under typical coating preparation conditions at ambient pressure and 60 °C for 6 h. The comparison between the two spectra indicates that solvents contributed mostly to a peak at 685 cm^{-1}. The observed triplet rather than a doublet or singlet band with maxima at 749, 788, and 809 cm^{-1} corresponds to different stretching modes of the two C–O bonds in each epoxide group and to the two diastereomeric groups of ECMA.[28] These assignments are supported by previous observations of the first two peaks in various epoxycyclohexyl compounds,[21,29] while the third has been noted in some epoxycyclohexyl-bearing copolymers.[21]

After photocuring, the triplet band between 718 and 835 cm^{-1} (marked by a cyan arrow) nearly disappeared, consistent with the consumption of the epoxide rings. Additionally, strong ether stretching peaks appeared between 1000 and 1125 cm^{-1} (marked by a yellow arrow), and the peaks between 1162 and 1252 cm^{-1} intensified, indicating the formation of new ether linkages.[30,31] A broad band, also marked by a yellow arrow, characteristic of hydroxyl groups appeared between 3000 and 3800 cm^{-1}. These hydroxyl groups are likely formed at the terminal ends of poly(cyclohexyloxide) chains (Scheme 1), resulting from the initiation reaction and water-induced termination reaction of cationic ring-opening polymerization of the 3,4-epoxycyclohexyl groups.[16] Overall, the ATR-FTIR data confirm the successful curing of the coating.

To obtain the epoxide conversion for the sample shown in Figure 4a, the area of the 788 cm^{-1} peak was integrated from 776 to 796 cm^{-1} and that of the C=O stretching peak of the ECMA ester group at 1724 cm^{-1} was integrated from 1644 to 1781 cm^{-1}. The decrease in the area ratio of these two peaks was used to calculate the epoxide conversion. For the particular sample shown in Figure 4a, the conversion was 85 ± 1%, where ±1% denotes the standard deviation and was obtained from repeating the baseline identification and area integration of the same two spectra three times.

Figure 4b shows how the hardness H of a 30 μm-thick F1 coating containing 5.0 wt % TSHFA varied with the photocuring time. The H value increased with curing time in

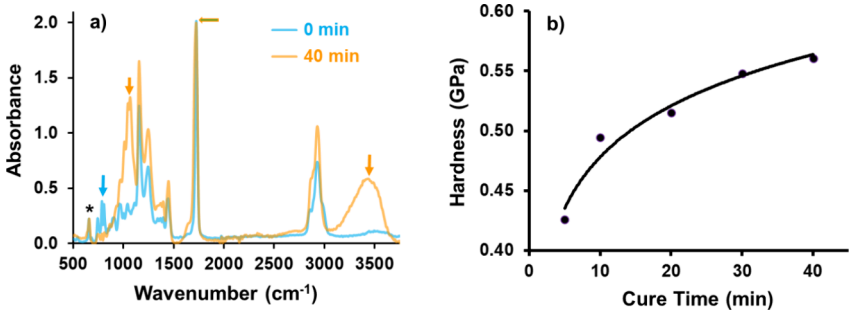

Figure 4. (a) Comparison of ATR-FTIR spectra of a 50 μm-thick F2 coating containing 5.0 wt % TSHFA before and after 40 min of photocuring. Panel (b) shows how the hardness H of a 30 μm-thick F1 coating varied as a function of photocuring time t.

https://doi.org/10.1021/acs.macromol.4c02127
Macromolecules 2024, 57, 11670–11678

the initial 30 min due to the cross-linking density increase but leveled off between 30 and 40 min. To maximize PECMA cross-linking, we photocured subsequently all coatings for 40 min unless mentioned otherwise.

We measured the conversions of four specimens for each sample photocured for 40 min. Table 2 presents the conversions for the various samples, along with their standard errors. The data suggest that epoxy conversions were high even when only 0.50% TSHFA was used. Despite this, the terminal epoxy conversion still increased slightly when the TSHFA amount was increased from 0.50 to 1.25%. Except F3, the conversions were mostly constant within experimental errors when the used TSHFA amounts increased from 2.0 and 5.0%. To maximize PECMA cross-linking, the used TSHFA amount was 5.0% by default unless mentioned otherwise.

Table 2. Effect of Varying the Photoinitiator Amount (PIA) on the Epoxy Conversion of Different Coatings

sample	PIA	epoxide conversion
F1	0.50	93 ± 1
	1.25	84 ± 1
	2.0	92 ± 1
	5.0	95 ± 2
F2	0.50	86 ± 1
	1.25	93 ± 3
	2.0	89 ± 1
	5.0	93 ± 2
F3	0.50	83 ± 3
	1.25	85 ± 2
	2.0	86 ± 1
	5.0	94 ± 2
F4	0.50	88 ± 2
	1.25	92 ± 1
	2.0	92 ± 2
	5.0	93 ± 2

Optical Transparency. Figure 5a shows a photograph of a cured F4 coating. The coating is highly transparent despite a yellow tint. This tint should have two contributions. First, the monomer ECMA and thus PECMA are slightly yellow, and second, the photoinitiator is also slightly yellow.

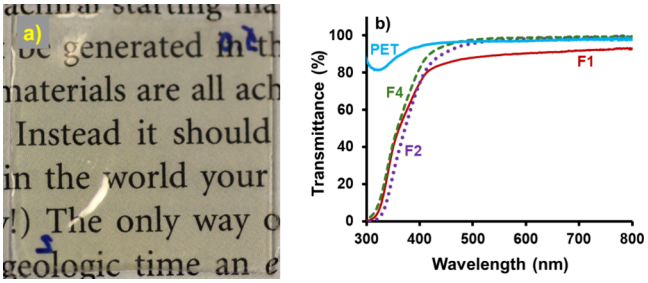

Figure 5. (a) Photograph of F4 coating photocured with 5.0% of the initiator placed on printed paper and (b) UV−visible transmittance spectra of several coatings. While all coatings were 50 μm-thick, the PET sample had a thickness of 125 μm, and a glass slide was used as the reference.

Figure 5b compares the transmittance spectra of three different coatings. PECMA samples exhibit some absorption below 500 nm, which contributes to their yellowish tone. Above 500 nm, the transmittances of the F2, F3, and F4 coatings are greater than 95%, whereas the F1 coating exhibits significantly lower transmittance. At 500 nm, the transmittance values for the coatings are 88.1% for F1 and 95.8, 98.0, and 97.8% for F2, F3, and F4, respectively. Notably, the F3 and F4 values exceed the 96.8% transmittance measured for a 125 μm-thick PET film.

The F1 coating shows substantially lower transmittance compared to the F2, F3, and F4 coatings. This reduction is likely due to the increased presence of cyano groups at the polymer chain ends, which may decrease the polymer's miscibility with the photoinitiator and result in phase separation. This separation could cause some cloudiness, which is noticeable when viewed under soft light.

Factors Affecting Nanoindentation Hardness and Other Properties. Coatings, 50 μm-thick, were prepared from F1−F4 with different TSHFA amounts, and they were then analyzed with a nanoindenter using different sample penetration depths. Some of these results are summarized in Table 3.

Table 3. Nanoindentation Hardness H, Effective Young's Modulus E, and Work Recovery w_e for Different Coating Samples Cured Using Different Photoinitiator Amounts PIA and Measured Using Different Nanoindenter Penetration Depths PD

sample	PIA	PD	H (GPa)	E (GPa)	w_e (%)
PET[a]	NA	7%	0.15 ± 0.01	0.45 ± 0.08	80 ± 2
PS[a]	NA	7%	0.23 ± 0.01	6.00 ± 0.20	19 ± 1
F1	2.0%	7%	0.50 ± 0.01	5.10 ± 0.08	37 ± 1
	5.0%	7%	0.54 ± 0.01	5.24 ± 0.09	37 ± 1
F2	2.0%	7%	0.66 ± 0.01	5.81 ± 0.06	41 ± 1
	5.0%	7%	0.62 ± 0.01	5.37 ± 0.02	43 ± 1
F3	0.50%	3%	0.62 ± 0.01	5.93 ± 0.07	39 ± 1
		5%	0.57 ± 0.01	5.71 ± 0.06	37 ± 1
		7%	0.57 ± 0.01	5.91 ± 0.03	36 ± 1
	1.25%	3%	0.73 ± 0.01	6.20 ± 0.02	44 ± 1
		5%	0.65 ± 0.01	5.87 ± 0.03	42 ± 1
		7%	0.66 ± 0.01	5.97 ± 0.03	41 ± 1
	2.0%	3%	0.71 ± 0.01	6.06 ± 0.03	44 ± 1
		5%	0.67 ± 0.01	5.94 ± 0.06	42 ± 1
		7%	0.66 ± 0.01	6.01 ± 0.05	41 ± 1
	5.0%	3%	0.78 ± 0.02	6.42 ± 0.09	45 ± 1
		5%	0.73 ± 0.01	6.10 ± 0.03	44 ± 1
		7%	0.70 ± 0.02	5.93 ± 0.20	42 ± 1
F4	2.0%	7%	0.68 ± 0.01	5.93 ± 0.06	45 ± 1
	5.0%	7%	0.68 ± 0.01	5.62 ± 0.04	45 ± 1

[a]Thicknesses of PET and PS films were 125 and 100 μm, respectively.

Nanoindentation hardness H has been of tremendous interest because higher H values can often be directly translated into greater wear resistance.[12] Additionally, an H/E ratio, with E denoting the effective Young's modulus, of greater than 10% and a work recovery w_e of higher than 60% have been cited as criteria for a hard coating to have flexibility.[32]

Data of Table 3 reveal several notable trends. First, PECMA coatings are exceptionally hard. For F3 coating, its H value reaches 0.70 ± 0.02 GPa measured using a penetration depth of 7%. This value is 4.7 ± 0.4 times the hardness of 0.15 ± 0.01 GPa for PET and 3.0 ± 0.2 times the hardness of 0.23 ± 0.01 GPa for PS measured under identical conditions. It significantly exceeds the 0.4 GPa hardness reported for the

https://doi.org/10.1021/acs.macromol.4c02127
Macromolecules 2024, 57, 11670−11678

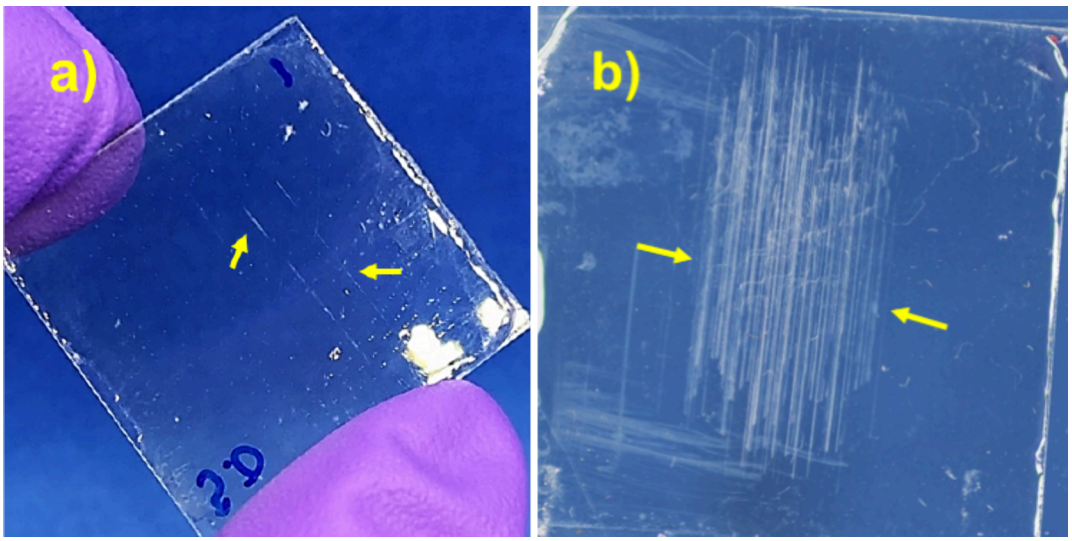

Figure 6. Photographs of (a) F4 coating after enduring 300 steel wool abrasion cycles as well as of (b) PS film cast on a glass plate after only a single abrasion cycle.

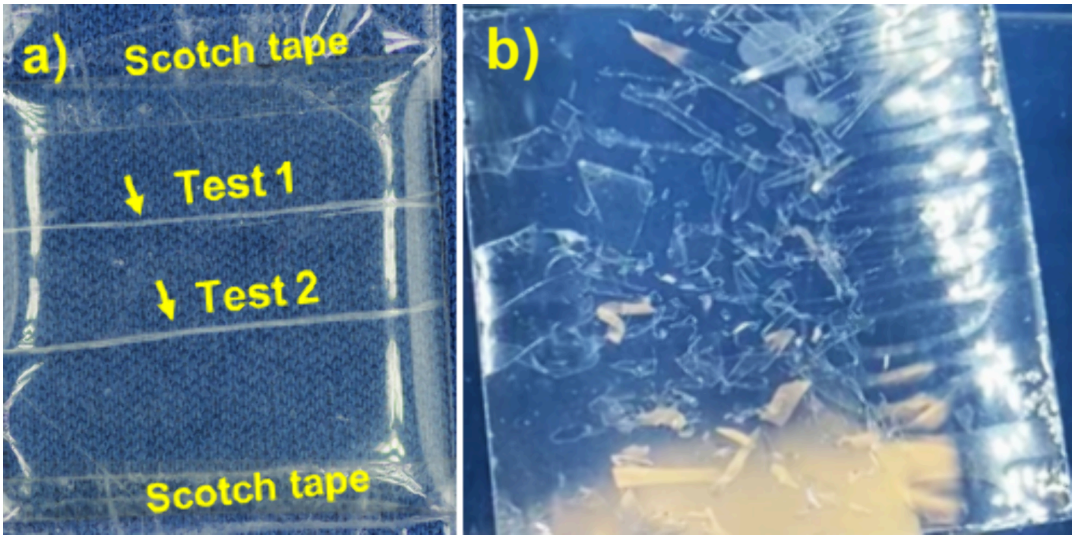

Figure 7. (a) Photograph of a 50 μm-thick F3 film after outward bending tests around a 2 mm-diameter steel rod at two different locations and (b) photograph of a 50 μm-thick PS film after one outward bending around a 20 mm-diameter steel rod. The F3 coating sample on PET rolled after bending tests, and the scotch tapes were used to flatten the sample on glass.

hardest organic polymer[1] and is the same as that reported for fully cured coating of 3-glycidyloxypropyl polyhedral oligomeric silsesquioxane (GPOSS),[10] an organic/inorganic molecular hybrid. A hardness of 0.70 GPa for a pure organic polymer coating is unprecedented.

Second, the H value increases initially with PECMA's molecular weight and then levels off after 14.5 kDa for F3. This molecular weight dependence of polymer properties is not unique and has been observed for many other properties such as glass transition temperature and Young's modulus.[33] The H value increases initially with PECMA molecular weight because the number of interchain bonds increases with the PECMA chain length. Above a critical molecular weight, other factors such as bond strength rather than the number of interchain bonds limits the hardness and other mechanical properties of the coating.

Third, the H/E values are close to 10% for the F1 coating and increase to ~12% as PECMA molecular weight increases. These values indicate that PECMA coatings can exhibit some flexibility. However, the w_e values for the F2−F4 coatings are only about 42%, which falls short of the >60% value required for adequate coating flexibility.[32]

Fourth, a slight decrease in H is observed with increasing sample penetration depth during nanoindentation measurements. This is a well-known phenomenon associated with the use of a Berkovich indenter, attributed to uncertainties in indentation area determination.[34] Although this effect is common, it is generally not pronounced. For samples F3 with 2.0 and 5.0 wt % TSHFA, H decreases by 0.05 and 0.08 GPa, respectively, when the penetration depth (PD) increases from 3 to 7%.

Fifth, the H values remain relatively constant with varying amounts of TSHFA, provided that the concentration is above 2.0 wt %. An exception is coating F2, where H decreased by 0.04 GPa, a difference small enough to be attributed to experimental error or potential variations in surface roughness.

https://doi.org/10.1021/acs.macromol.4c02127
Macromolecules 2024, 57, 11670−11678

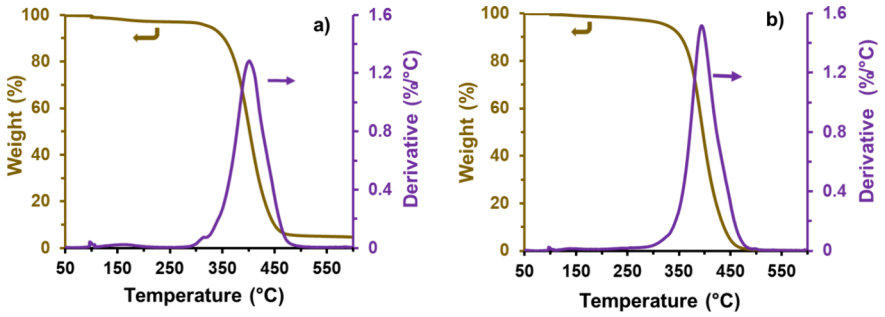

Figure 8. TGA curve for F3 containing 5.0 wt % of TSHFA (a) before and (b) after 40 min of photocuring.

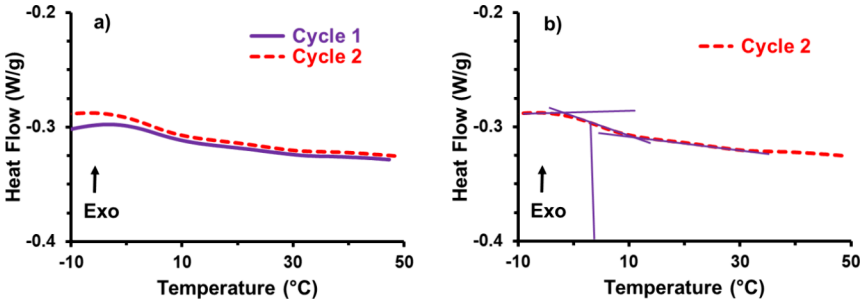

Figure 9. Panel (a) presents DSC heating curves from the first and second thermal cycles for a photoinitiator-free F3 sample. Panel (b) highlights the determination of T_g from the second heating curve.

Abrasion Resistance. An F4 coating at a thickness of 50 μm was abraded with steel wool under a nominal pressure of 13 kPa. After 250 cycles, no visible scratches were observed on the coating. Between 250 and 300 cycles, abraded lines, as marked by arrows in Figure 6a, appeared on the surface of the coating. This contrasts with PS, which developed defined lacerations after a single abrasion cycle, Figure 6b. Therefore, the high hardness of PECMA coating translates directly into superb wear resistance.

Bendability. F1 and F3 coating samples, each 50 μm-thick, were prepared on 50 μm-thick PET films and subjected to bending tests. During these tests, the bilayer samples were wrapped around steel rods with the coatings facing inward toward the rod. Even when using the smallest 2 mm-diameter steel rod provided by the instrument manufacturer, no cracking or detachment of the samples was observed. Thus, both coatings feature an inward bending diameter of 2 mm and possibly smaller.

When the coating samples were wrapped around steel rods with PET in contact with the rods, no damage was observed if the rod's diameter was 4 mm or larger. However, when the diameter was reduced to 3 mm, both F1 and F3 coatings developed fault lines. Figure 7a illustrates an F3 coating sample subjected to two outward bending tests around a 3 mm rod at different locations, with arrows indicating the fault lines. These observations suggest that the outward bending diameter for these coatings is 4 mm.

Typically, hard materials exhibit greater outward bending diameters than inward bending diameters because outward bending involves elongation of the material, whereas inward bending involves compression. Generally, hard materials can better tolerate compression than elongation.[35]

The outward bending diameter of 4 mm for a 50 μm-thick film is relatively low. Previously studied organic/inorganic hybrid coatings of similar thickness typically had an outward bending diameter of 5 mm or more.[12,36] Thus, PECMA coatings demonstrate better bendability than earlier hybrid coatings. The work recovery values for these coatings, as determined by nanoindentation analysis and reported in Table 3, are below 60%. This suggests that the >60% work recovery criterion for hard/flexible coatings may be somewhat arbitrary,[32] especially given that the specific criteria for coating flexibility are not clearly defined.

Figure 7b also shows a 50 μm-thick PS coating on PET after it underwent outward bending around a 20 mm-thick rod. The PS coating fractured into pieces, revealing PS's brittleness. Previously, inward and outward bending diameters of 10 mm and >32 mm were determined for PS of this thickness.[12] Therefore, cured PECMA is a unique hard yet flexible organic polymer.

Thermal Properties. Figure 8 compares TGA curves for the F3 sample before and after photocuring. The two sets of curves are very similar, experiencing <3.0% mass loss at 250 °C probably due to evaporation of residual solvents and initiator fragments. Major weight losses are observed only above 390 °C, corresponding to polymer decomposition.[37] Therefore, both cured and noncured PECMA are thermally quite stable.

Figure 9a compares the DSC heating curves from the first and second thermal cycles for a photoinitiator-free F3 sample, both showing a step. Figure 9b identifies the glass transition temperature (T_g) at ~4 °C, explaining PECMA's viscous liquid state at room temperature. In contrast, Figure S3a shows two DSC heating curves for cross-linked F3 between −20 and 100 °C. The first curve reveals a T_g of ~46 °C, while the second shows no T_g up to 100 °C. The disappearance of T_g from the second curve may be due to solvent evaporation and increased cross-linking during the first heating ramp, reducing chain mobility and raising the T_g beyond 100 °C.

Water Contact Angles. The water contact angles of F1, F2, F3, and F4 coatings are 84 ± 1, 76 ± 1, 77 ± 1, and 76 ± 1°, respectively. Thus, PECMA is moderately hydrophobic. The fact that the F1 coating features a higher water contact

https://doi.org/10.1021/acs.macromol.4c02127
Macromolecules 2024, 57, 11670−11678

angle than the other coatings is most likely due to the increased concentration of methyl groups in the isobutylnitrile end groups in F1. Methyl groups are quite hydrophobic and can increase the water contact angle of the PECMA coating.[38,39]

CONCLUSIONS

The bifunctional monomer ECMA was polymerized using free radical polymerization in THF to yield a linear polymer. The polymer was further fractionated into samples with M_w values of 4.1, 9.3, 14.5, and 29.9 kDa. PECMA and its fractions are viscous liquids at room temperature.

PECMA after photocuring with the cationic photoinitiator TSHFA became a solid. The nanoindentation hardness (H) and effective Young's modulus (E) of the coatings initially increased with PECMA M_w but plateaued above 14.5 kDa. Increasing the TSHFA concentration enhanced E and H values when the amount was below 2.0 wt %, but no significant changes were observed when the concentration was increased from 2.0 to 5.0 wt %. The F3 coating, cured with 2.0 or 5.0 wt % TSHFP, demonstrated H values five times greater than PET and three times greater than PS. The F4 coating withstood 250 cycles of abrasion with steel wool under a nominal pressure of 13 kPa without visible damage. Aside from exceptional hardness and wear resistance, photocured PECMA coating on a PET support film exhibited impressive flexibility, with an inner bending diameter of 2 mm and an outward bending diameter of 4 mm. The F2−F4 coatings, each 50 μm-thick, remained highly transparent with a transmittance close to 98% at 500 nm. PECMA also displayed excellent thermal stability, with no appreciable degradation below 300 °C. The various fascinating properties of PECMA and its cured resin suggest that the polymer has significant potential for applications in coatings, dental materials, sealants, and adhesives.

ASSOCIATED CONTENT

Supporting Information

The Supporting Information is available free of charge at https://pubs.acs.org/doi/10.1021/acs.macromol.4c02127.

Experimental details concerning glass slide pretreatment and techniques for various analyses including SEC, NMR, nanoindentation, contact angle, ATR-FTIR, abrasion, transmittance, bendability, TGA, and DSC (PDF)

AUTHOR INFORMATION

Corresponding Author

Guojun Liu − *Department of Chemistry, Queen's University, Kingston, Ontario K7L 3N6, Canada;* orcid.org/0000-0002-9643-5070; Email: gliu@chem.queensu.ca

Authors

Ryan Seck − *Department of Chemistry, Queen's University, Kingston, Ontario K7L 3N6, Canada*

Ziruo Lai − *Department of Chemistry, Queen's University, Kingston, Ontario K7L 3N6, Canada*

Complete contact information is available at: https://pubs.acs.org/10.1021/acs.macromol.4c02127

Notes

The authors declare no competing financial interest.

ACKNOWLEDGMENTS

We gratefully acknowledge NSERC Canada for funding this research, and GL extends thanks to the Canada Research Chairs Program for the Tier I position in materials science.

REFERENCES

(1) Xu, J.; Asatekin, A.; Gleason, K. K. The Design and Synthesis of Hard and Impermeable, yet Flexible, Conformal Organic Coatings. *Adv. Mater.* **2012**, *24*, 3692−96.

(2) Alisafaei, F.; Han, C. S. Indentation Depth Dependent Mechanical Behavior in Polymers. *Adv. Condens. Matter Phys.* **2015**, *2015*, No. 391579.

(3) Pendhari, S. S.; Kant, T.; Desai, Y. M. Application of Polymer Composites in Civil Construction: A General Review. *Compos. Struct.* **2008**, *84*, 114−24.

(4) Ye, L.; Lu, Y.; Su, Z.; Meng, G. Functionalized Composite Structures for New Generation Airframes: A Review. *Compos. Sci. Technol.* **2005**, *65*, 1436−46.

(5) Gibson, R. F. A Review of Recent Research on Mechanics of Multifunctional Composite Materials and Structures. *Compos. Struct.* **2010**, *92*, 2793−810.

(6) Bender, D. N.; Liu, G. Endowment of Omniphobicity and Exceptional Bendability to a Wear-Resistant Poss Coating. *Chem. Eng. J.* **2023**, *464*, No. 142702.

(7) Tan, S. C. K.; Liu, G. Free-Standing Flexible Composite Film That Is Transparent, Omnipohobic, and Resistant against Steel Wool Abrasion. *ACS Appl. Polym. Mater.* **2024**, *6*, 504−14.

(8) Zhang, Z. Q.; Huang, Y. J.; Xie, Q. Y.; Liu, G. J.; Ma, C. F.; Zhang, G. Z. Functional Polymer-Ceramic Hybrid Coatings: Status, Progress, and Trend. *Prog. Polym. Sci.* **2024**, *154*, No. 101840.

(9) Zvonkina, I. J.; Soucek, M. D. Inorganic-Organic Hybrid Coatings: Common and New Approaches. *Curr. Opin. Chem. Eng.* **2016**, *11*, 123−27.

(10) Zhang, K.; Huang, S.; Wang, J.; Liu, G. Transparent Omniphobic Coating with Glass-Like Wear Resistance and Polymer-Like Bendability. *Angew. Chem., Int. Ed.* **2019**, *58*, 12004−09.

(11) Choi, G.-M.; Jin, J.; Shin, D.; Kim, Y. H.; Ko, J.-H.; Im, H.-G.; Jang, J.; Jang, D.; Bae, B.-S. Flexible Hard Coating: Glass-Like Wear Resistant, yet Plastic-Like Compliant, Transparent Protective Coating for Foldable Displays. *Adv. Mater.* **2017**, *29*, No. 1700205.

(12) Bender, D. N.; Hait, S.; Lichtenhan, J. D.; Liu, G. Uv Curing Behavior of Five Heteroleptic Poss Bearing Methacrylate and Glycidyl Groups and Evaluation of Their Potential for Hard yet Flexible Coatings. *ACS Appl. Polym. Mater.* **2022**, *4*, 1878−89.

(13) Bender, D. N.; Zhang, K.; Wang, J.; Liu, G. Hard yet Flexible Transparent Omniphobic Gposs Coatings Modified with Perfluorinated Agents. *ACS Appl. Mater. Interfaces* **2021**, *13*, 10467−79.

(14) Lai, Z.; Liu, G. Facile Preparation of a Transparent and Rollable Omniphobic Coating with Exceptional Hardness and Wear Resistance. *ACS Appl. Mater. Interfaces* **2022**, *14*, 35138−47.

(15) Lai, Z.; Song, N.; Benmeddour, A.; Liu, G. Lubricated Pdms-Bearing Ladderlike Polysilsesquioxane Coating: Fabrication and Factors Governing Its Long-Term Ice-Shedding Performance. *Chem. Eng. J.* **2024**, *484*, No. 149698.

(16) Crivello, J. V.; Lam, J. H. W. Photoinitiated Cationic Polymerization Wtih Triarylsulfonium Salts. *J. Polym. Sci: Part A: Polym. Chem.* **1979**, *17*, 977−99.

(17) Kuwana, A.; Honda, K.; Koga, K. A Process for the Preparation of a Purified 3,4-Epoxycyclohexyl-Methyl (Meth)Acrylate. European Patent Office EP0529197B1, 1998.

(18) Suzuki, H.; Nakai, Y. High Purity 3,4-Epoxycyclohexylmethyl Methacrylate. ROC Patent TW202035381A, 2020.

(19) Liu, Y.; Palasz, P.; Paul, C. W.; Foreman, P. B. Cationic Uv-Crosslinkable Acrylic Polymers for Pressure Sensitive Adhesives. US8796350B2, 2014.

(20) Yamawake, K.; Hayashi, M. The Role of Tertiary Amines as Internal Catalysts for Disulfide Exchange in Covalent Adaptable Networks. *Polym. Chem.* **2023**, *14*, 680−86.

(21) Lu, M. P.; Liu, Y. C.; Liang, L. Y.; Lu, M. G. Synthesis and Characterization of Easily Degradable Acrylate-Epoxy Resin with Superior Dielectric Properties and High Transmittance. *Polymer* **2020**, *202*, No. 122711.
(22) He, Y.; Xiao, M.; Wu, F.; Nie, J. Photopolymerization Kinetics of Cycloaliphatic Epoxide-Acrylate Hybrid Monomer. *Polym. Int.* **2007**, *56*, 1292−97.
(23) Fox, T. G.; Gratch, S. Crosslinking in Monovinyl Monomers 0.1. By Chain Transfer with the Polymer Chain. *Ann. N.Y. Acad. Sci.* **1953**, *57*, 367−83.
(24) Young, R. J. L. P. A., *Introduction to Polymers*. 2nd Ed. Chapman&Hall: London, 1991.
(25) Wolpert, A.; Lai, Z.; Wu, G.; Liu, G. Synthesis of Mixed Ladder-Like Polysilsesquioxanes by Copolymerization of 2-(3,4-Epoxycyclohexyl)Ethyltrimethoxysilane and Dodecyltrimethoxysilane. *Macromolecules* **2024**, *57*, 5838−48.
(26) Ward, A. J.; Lesic, R. A.; Proschogo, N.; Masters, A. F.; Maschmeyer, T. Strained Surface Siloxanes as a Source of Synthetically Important Radicals. *RSC Adv.* **2015**, *5*, 100618−24.
(27) Almeida, A. R.; Moulijn, J. A.; Mul, G. In Situ Atr-Ftir Study on the Selective Photo-Oxidation of Cyclohexane over Anatase Tio2. *J. Phys. Chem. C* **2008**, *112*, 1552−61.
(28) Smith, B. C. The Infrared Spectra of Polymers V: Epoxies. *Spectroscopy* **2022**, *37*, 17−18.
(29) Kim, Y. M.; MacGregor, J. F.; Kostanski, L. K. Principal Component Analysis of Ft-Ir Spectra for Cationic Photopolymerization of Mixtures of Two Monomers. *Chemom. Intell. Lab. Syst.* **2005**, *75*, 77−90.
(30) Cai, Y.; Jessop, J. L. P. Decreased Oxygen Inhibition in Photopolymerized Acrylate/Epoxide Hybrid Polymer Coatings as Demonstrated by Raman Spectroscopy. *Polymer* **2006**, *47*, 6560−66.
(31) Bec, K. B.; Grabska, J.; Ozaki, Y.; Hawranek, J. P.; Huck, C. W. Influence of Non-Fundamental Modes on Mid-Infrared Spectra: Anharmonic Dft Study of Aliphatic Ethers. *J. Phys. Chem. A* **2017**, *121*, 1412−24.
(32) Musil, J. Flexible Hard Nanocomposite Coatings. *RSC Adv.* **2015**, *5*, 60482−95.
(33) Torres, J. M.; Stafford, C. M.; Vogt, B. D. Impact of Molecular Mass on the Elastic Modulus of Thin Polystyrene Films. *Polymer* **2010**, *51*, 4211−17.
(34) Zhu, P.; Zhao, Y.; Agarwal, S.; Henry, J.; Zinkle, S. J. Toward Accurate Evaluation of Bulk Hardness from Nanoindentation Testing at Low Indent Depths. *Mater. Des.* **2022**, *213*, No. 110317.
(35) Gleskova, H.; Wagner, S.; Suo, Z. Failure Resistance of Amorphous Silicon Transistors under Extreme in-Plane Strain. *J. Appl. Phys.* **1999**, *75*, 3011−13.
(36) Moreno, I.; Navascues, N.; Arruebo, M.; Irusta, S.; Santamaria, J. Facile Preparation of Transparent and Conductive Polymer Films Based on Silver Nanowire/Polycarbonate Nanocomposites. *Nanotechnol.* **2013**, *24*, 275603.
(37) Koga, N.; Vyazovkin, S.; Burnham, A. K.; Favergeon, L.; Muravyev, N.; Pérez-Maqueda, L. A.; Saggese, C.; Sánchez-Jiménez, P. E. Ictac Kinetics Committee Recommendations for Analysis of Thermal Decomposition Kinetics. *Thermochim. Acta* **2023**, *719*, No. 179384.
(38) Ignat'ev, N. V.; Finze, M.; Sprenger, J. A. P.; Kerpen, C.; Bernhardt, E.; Willner, H. New Hydrophobic Ionic Liquids with Perfluoroalkyl Phosphate and Cyanofluoroborate Anions. *J. Fluorine Chem.* **2015**, *177*, 46−54.
(39) Wang, Z. H.; Yu, C.; Zhao, J. F.; Guo, P.; Liu, H. Molecular Dynamics Simulation for Quantitative Characterization of Wettability Transition on Silica Surface. *JMR&T* **2022**, *19*, 4371−80.

https://doi.org/10.1021/acs.macromol.4c02127
Macromolecules 2024, 57, 11670−11678